Properties of surface wave trains excited by mass transfer through a liquid surface

A. Wierschem,[1,2] H. Linde,[2,3] and M. G. Velarde[2]
[1]*LS Technische Mechanik und Strömungsmechanik, Universität Bayreuth, D-95440 Bayreuth, Germany*
[2]*Instituto Pluridisciplinar, Paseo Juan XXIII, No. 1, E-28040 Madrid, Spain*
[3]*Straße 201 Nr. 6, D-13156 Berlin, Germany*
(Received 17 January 2001; published 19 July 2001)

In annular containers, various traveling periodic surface wave trains are generated in liquid layers during the absorption process of a miscible surface-active substance out of the vapor phase. Single and counter-rotating wave trains are observed. We here report on waves found to be dispersion-free associated to mostly longitudinal, dilational surface-tension-gradient-driven motions. We report on interactions of the wave crests and on modulations that lead to wave-number changes of the wave trains. The wave interactions show behavior typically known for solitons.

DOI: 10.1103/PhysRevE.64.022601 PACS number(s): 47.20.Dr, 47.54.+r

In Bénard-Marangoni convection, when a liquid layer is heated from below, the temperature dependence of surface tension generally produces a stationary, hexagonal convective pattern [1–3]. In liquids that are heated from the side, so-called hydrothermal waves and surface waves are observed [4–6]. In annular containers, waves may appear rotating perpendicularly to the applied temperature gradient. Various types of surface waves have also been observed in mass-transfer-driven experiments [7]. In the latter, a liquid absorbs a vapor that lowers the surface tension as the temperature does in heat-transfer experiments. Heating from above has also been studied in annular containers. It also leads to the excitation of wave trains [8]. The equivalent mass-transfer-driven system has been studied in different geometries and with a variety of substances [9–13].

Various properties of the waves generated with a vertical concentration gradient have been reported. Their solitonic behavior has been established by following oblique crest and head-on collisions and wall reflections at various angles [11,12]. It was also found that the form of the container has a strong influence on the selected wave pattern [13]. Here, we report on single and counter-rotating two-dimensional wave trains in annular-ring containers. We provide the dispersion relation of these surface waves and compare it to theoretical predictions. We also report here on the modulations of wave trains. These modulations lead to wave-number changes of the wave trains. They reveal an energy exchange between neighboring crests, which is typical for solitons. Furthermore, we show how counter-rotating trains adjust their wave number by a switching of the extinction process between the two wave trains.

A side view of the setup is sketched in Fig. 1. It consists of a cylindrical glass container of 190 ± 1 mm diameter in which two quartz rings of 10.45 ± 0.05 mm height are placed concentrically. The inner ring of 50.05 ± 0.05 mm diameter and the outer one of 74.50 ± 0.05 mm diameter are concentric within 1%. The annular gap between the two quartz rings is filled with toluene. The rest of the container is covered with liquid pentane, which has a high vapor pressure at room temperature and a surface tension much lower than toluene. Furthermore, its density and viscosity are much lower than that of toluene. The characteristic parameters are given in Table I [14]. See [7] for further details about the characteristic parameters of the chemicals. Because the surface level rises due to the absorbed pentane, the annular container was not filled brimful. The experiment starts by uncovering the annular ring, leaving the toluene surface open to the pentane vapor. The experimental runs are carried out with the reservoir open to the ambient air at temperatures between 299.75 and 300.05 K. The waves have been visualized with the shadowgraph method using a monochromatic light beam.

The vapor concentration of pentane rises rapidly until it reaches a stationary value, which is governed by the equilib-

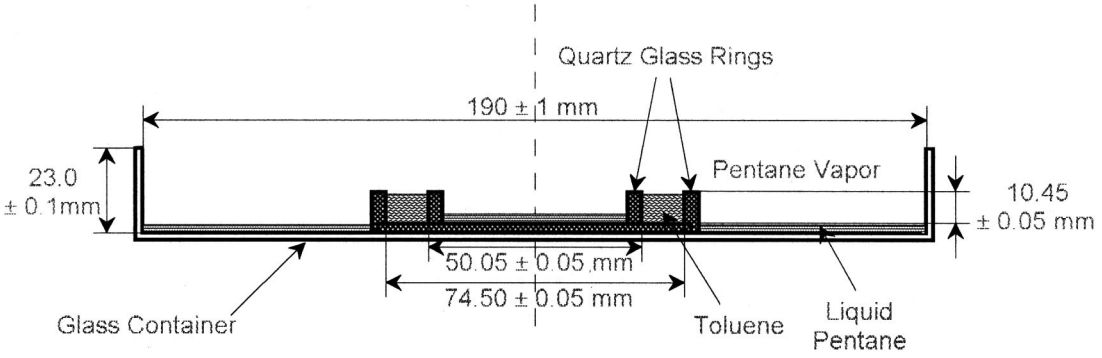

FIG. 1. Side view of the experimental setup: two quartz-glass rings form an annular container that is placed concentrically in a circular reservoir made of glass. The annular ring is filled with toluene and the bottom of the reservoir is covered with liquid pentane.

TABLE I. Properties of liquid toluene and liquid pentane [14].

Properties	Liquid toluene	Liquid pentane
Molecular weight u (g/mol)	92.15	72.15
Boiling point T_B (K)	383.75	309.22
Density ρ at 293.15 K (g/cm^3)	0.8669	0.6262
Refraction index n at sodium D line	1.4961	1.3575
Surface tension σ at 298.15 K (mN/m)	27.93	15.49
Dynamic viscosity η at 298.15 K (mPa/s)	0.560	0.224

rium between the evaporating and the outward diffusing pentane. The strong concentration difference between the vapor phase and the liquid governs the absorption process of pentane. Since the absorbed pentane remains in the liquid, the experiment is instationary by its nature. At high concentration differences between the vapor and the liquid, the absorption becomes so strong that the concentration gradient at the liquid surface cannot be maintained for a long period. However, we were able to have wave trains lasting for about 100 to 200 s. During this time, they adjust their wavelength to the diminishing concentration gradient at the liquid surface. Finally, they loose stability in favor for internal waves [15].

In our instationary experiment, except for an initial stage, the wave number of the wave trains decreases with time. We have observed trains made up of 8–13 wave crests. The frequency of the wave trains, as averaged over the time it takes to circumvent once the entire container, increases with the wave mode, as shown in Fig. 2. Within the uncertainty, the linear fit to the frequency f goes through zero: $f=0.007 \pm 0.053\,\mathrm{Hz}+0.095\pm 0.005\,\mathrm{Hz}\times[n]$, where $[n]$ is the wave mode, and hence $[n]$ accounts for the nearest integral number. The phase velocity is about 19 mm s^{-1}. Thus within the uncertainty of the measurement, the two-dimensional waves are dispersion-free. This is in accordance with theoretical descriptions of longitudinal surface waves [16–18].

For further comparison of our experimental data with the theoretical findings by Rednikov *et al.* [17,18], we note that in the theory, the vertical concentration gradient is assumed

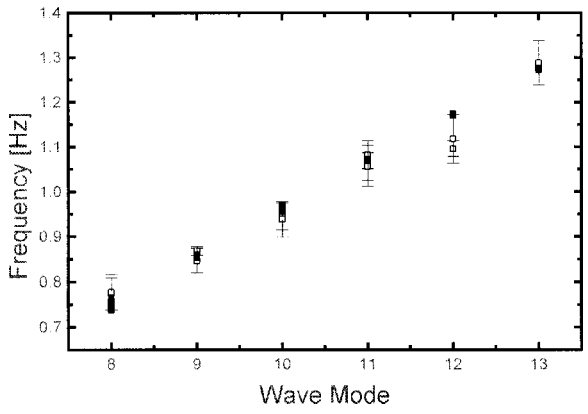

FIG. 2. Mean frequency as a function of the wave mode. The theoretical values are indicated by solid squares and the experimental values by open squares. The error bars indicate the maximum and minimum values observed.

to be constant, although this is not the case in the experiment. However, we may focus on the concentration gradient near enough to the liquid surface. Since the pentane in the gas phase can be replaced much faster than it can be carried away from the surface on the liquid side, we may assume that there is an equilibrium pentane concentration close to the surface on the air side. Then, the vertical concentration gradient can be set equal to that of the liquid bulk. Assuming further that there is constant mixing along the convective liquid layer, the pentane concentration can be written as:

$$c(z)=c_s\left[1-\exp\left(-\frac{z}{z_0}\right)\right], \tag{1}$$

where c_s is the pentane concentration close to the surface on the air side. z_0 is the scale of the vertical concentration gradient in the liquid. Close to the surface this reduces to

$$\frac{dc}{dz}\approx\frac{c_s}{z_0}. \tag{2}$$

Experiments show that the convective flow motion associated to the waves is almost entirely restricted to the upper 4.5 mm of the liquid layer. Fitting the measured concentration gradient in this region to experimental data yields $z_0 \approx 1.5\,\mathrm{mm}$. The concentration in the vapor side can be obtained by comparing the measured absorption rate to that achieved when the saturation concentration is reached. It turns out that it is about a third of the saturation concentration. Taking into account the approximation made in Eq. (2), the dispersion relation at leading order according to theory [16–18] can be written in dimensional form:

$$f=\sqrt{-\frac{d\sigma}{dc_s}\frac{c_s}{z_0}\frac{1}{\rho_s}\frac{1}{\sqrt{\mathrm{Sc}}-1}}\,\frac{1}{L}n, \tag{3}$$

where f, ρ_s, $\mathrm{Sc}=\eta_s/\rho_s D$, L, n are frequency, density at the surface, Schmidt number, mean circumference length of the annular ring, and the number of waves in the container, respectively. The dependence of the parameters on the pentane concentration is given in [7]. The theoretical values are compared to the experimental data in Fig. 2. The theoretical values are in good agreement despite the approximations made. We remark that with the definition [17,18] using the effective liquid depth z_0 the Marangoni number, $M=-(d\sigma/dc_s)(c_s z_0/\eta_s D)$, is about 3×10^6. In our instationary experiment, it decreases exponentially with time. On the other hand, the time a train of certain wave number exists increases roughly exponentially with time (for an illustration, see Fig. 5).

The wave trains show modulations, which lead to the disappearance of single wave crests. The wave number changes by head-on interaction between crests that travel *in the same direction*. Figure 3 shows an example of this process. The figure also reveals that counter-rotating crests have no major impact on the extinction process. The process starts by a localized modulation. First, a single crest slows down. At the same time, the contrast in the shadowgraph image reduces. The next crest behind catches up without diminishing its velocity. Being close to the slower one, the amplitude of the

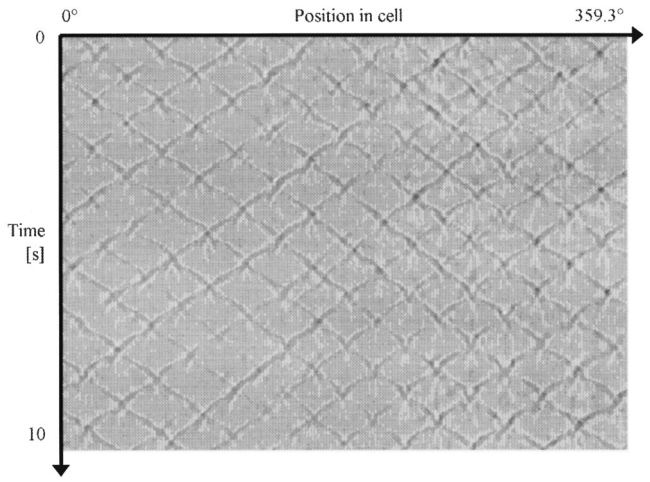

FIG. 3. Space-time diagram of the modulation in a system of two counter-rotating wave trains. The modulation travels from the upper right to the lower left. $T=300.05$ K.

faster crest, seen as the contrast in the shadowgraph image, increases. Thereafter, at a characteristic distance between the two crests, the slower crest accelerates and now its amplitude increases. Distances between 4.6 ± 0.6 mm and 5.7 ± 0.7 mm have been observed. The faster crest begins now to lag behind and its amplitude decreases. Its neighbor behind comes up and the process repeats. This interactive region moves through the container from one wave crest to the next until one crest is caught up by its neighbor but cannot recover and disappears.

As can be seen in Fig. 3, the modulations travel slower than the phase velocity of the underlying waves but in the same direction. The modulation velocity as a function of the wave mode is displayed in Fig. 4. It is measured as the average velocity during the whole time the modulation is observed. Figure 4 indicates that the modulation velocity decreases with the wave mode. The linear fit yields for the modulation velocity: $v_M=19.23\pm0.24\,\mathrm{mm\,s^{-1}}-0.50\pm0.02\,\mathrm{mm\,s^{-1}}\times[n]$. Thus, within the uncertainty, at mode zero the extrapolation of the linear fit yields for the modulation velocity the same value as for the phase velocity of the waves.

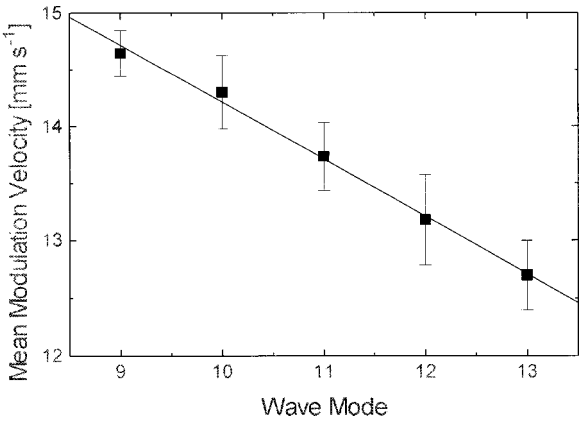

FIG. 4. Velocity of the traveling modulations.

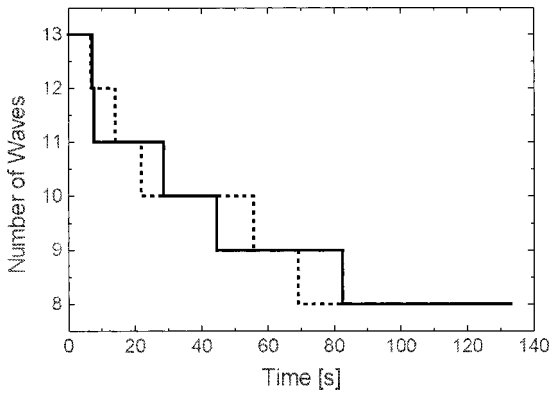

FIG. 5. Number of waves of an experimental run with counter-rotating wave trains as a function of time. Values of the left-moving crests are depicted as a dotted line and the right-traveling train as a solid one. The time of existence of each new wave train is longer than the time of its predecessor. Each time one train has one wave less than the other, the other is the next to lose one wave to equal the number of waves and another one to which the first train is going to equalize by losing one wave, $T=300.05$ K.

In an idealized model, the wave crests can be considered as spheres of an extension of $\lambda_0=L/_{38}\approx5.2$ mm, which corresponds to the minimum distance of two wave crests during modulation, that interact by inelastic collisions. Between the collisions, they cover the remaining free surface without the crests in the same time as if they that were covering the entire container by traveling at phase velocity: $v_M=(L-n\lambda_0/L)v_P$.

The head-on collisions of the crests of counter-rotating wave trains have been studied earlier [11–13]. They show a change of trajectory with negative phase-shift typical for solitons and shock waves [19–21]. The counter-rotating wave trains loose single crests as a result of modulations in the same way as single wave trains. The disappearance of a single wave crest, however, is not arbitrary in the regime of counter-rotating wave trains. The trains show alternation of the wave number of each train during the experimental run. Figure 5 presents an example. Each time one train has one wave crest less than the other, the latter is the next to loose one wave to match the number of waves of the former. But it also looses the next wave, thus loosing two crests in a row. Thereafter, the other train looses two wave crests. In this manner the trains interchange in having fewer wave crests than the other. Each new train of lower wave mode exists longer than its predecessor.

The switching of disappearing wave crests between the counter-rotating wave trains may be understood qualitatively taking into account that the waves are dispersion free: Due to the decreasing Marangoni number, the wave number of both trains must adjust. The first adjustment is arbitrary and arises from erratic fluctuations. Then, one train has one wave crest more than the other. As time proceeds, it also has to adjust its wavelength to the decreasing Marangoni number, while the other train with lower wave number can relax from the inhomogeneous state caused by the missing wave crest. Hence, after a while; the train with a higher wave number looses a wave to attain the number of the other train. But

when another wave crest has to disappear due to the further decreasing Marangoni number, this train is still less homogeneous than the train that lost a wave before. Since in the inhomogeneous wave train the local wave number is lowest in some region, the feeding of pentane cannot sustain the two neighboring waves. As a consequence, localized modulations set in that lead to the disappearance of a further wave crest. As time proceeds, this mechanism repeats for the other wave train. Thus, the essential feature for the switching between the wave trains is the slow disappearance of inhomogeneities in the wave trains due to their dispersion-free character.

In conclusion, surface waves generated in annular containers in liquid layers during the absorption process of a miscible surface-active substance out of the vapor phase form two-dimensional traveling periodic wave trains. They are found to be essentially dispersion free in agreement with theory [16–18]. Wave-train modulations lead to wave-number changes of the wave trains with an energy exchange at minimum distance between neighboring crests typical for solitonic waves. Counter-rotating trains adjust their wave number by the switching of the extinction process.

A.W. gratefully acknowledges financial support by the Gottlieb Daimler und Karl Benz-Stiftung. This research has also been supported by the Spanish Ministry of Education and Culture under Grant No. DGICYT PB96-0599 and by the European Union under ICOPAC Network Grant No. HPRN-CT-2000-00136.

[1] M. J. Block, Nature (London) **178**, 650 (1956).
[2] E. L. Koschmieder, *Bénard Cells and Taylor Vortices* (Cambridge University, Cambridge, England, 1994).
[3] M. G. Velarde, A. A. Nepomnyashchy, and M. Hennenberg, Adv. Appl. Mech. **37**, 167 (2000).
[4] D. Schwabe, U. Möller, J. Schneider, and A. Scharmann, Phys. Fluids A **4**, 2368 (1992).
[5] J. Schneider, D. Schwabe, and A. Scharmann, Microgravity Sci. Technol. **9/2**, 86 (1996).
[6] S. H. Davis, Annu. Rev. Fluid Mech. **19**, 403 (1987).
[7] A. Wierschem, M. G. Velarde, and H. Linde, J. Colloid Interface Sci. **212**, 365 (1999).
[8] L. Weh and H. Linde, J. Colloid Interface Sci. **187**, 159 (1997).
[9] H. Linde, E. Schwarz, and K. Gröger, Chem. Eng. Sci. **22**, 823 (1967).
[10] P. D. Weidman, H. Linde, and M. G. Velarde, Phys. Fluids A **4**, 921 (1992).
[11] H. Linde, X-L. Chu, and M. G. Velarde, Phys. Fluids A **5**, 1068 (1993).
[12] H. Linde, X.-L. Chu, M. G. Velarde, and W. Waldhelm, Phys. Fluids A **5**, 3162 (1993).
[13] H. Linde, M. G. Velarde, A. Wierschem, W. Waldhelm, K. Loeschcke, and A. Ye. Rednikov, J. Colloid Interface Sci. **188**, 16 (1997).
[14] *CRC Press, Inc. Handbook of Chemistry and Physics*, 76th ed., edited by D. R. Lide (CRC, West Palm Beach, FL, 1996).
[15] A. Wierschem, H. Linde, and M. G. Velarde, Phys. Rev. E **62**, 6522 (2000).
[16] X.-L. Chu and M. G. Velarde, PhysicoChem. Hydrodyn. **10**, 727 (1988).
[17] A. Ye. Rednikov, P. Colinet, M. G. Velarde, and J. C. Legros, J. Fluid Mech. **405**, 57 (2000).
[18] A. Ye. Rednikov, P. Colinet, M. G. Velarde, and J. C. Legros, J. Non-Equilib. Thermodyn. **25**, 381 (2000).
[19] N. J. Zabusky and M. D. Kruskal, Phys. Rev. Lett. **15**, 240 (1965).
[20] R. Courant and K. O. Friedrichs, *Supersonic Flow and Shock Waves* (Interscience, New York, 1948).
[21] C. H. Su and R. M. Mirie, J. Fluid Mech. **98**, 509 (1980).